UC Berkeley
UC Berkeley Previously Published Works

Title

Warming promotes loss of subsoil carbon through accelerated degradation of plant-derived organic matter

Permalink

https://escholarship.org/uc/item/4b22j4d8

Authors

Ofiti, Nicholas OE
Zosso, Cyrill U
Soong, Jennifer L
et al.

Publication Date

2021-05-01

DOI

10.1016/j.soilbio.2021.108185

Peer reviewed

Warming promotes loss of subsoil carbon through accelerated degradation of plant-derived organic matter

Nicholas O.E. Ofiti [a,*], Cyrill U. Zosso [a], Jennifer L. Soong [b], Emily F. Solly [a,c], Margaret S. Torn [b], Guido L.B. Wiesenberg [a], Michael W.I. Schmidt [a]

[a] Department of Geography, University of Zurich, Zurich, Switzerland
[b] Climate and Ecosystem Science Division, Earth and Environmental Science Area, Lawrence Berkeley National Laboratory, Berkeley, CA, USA
[c] Group for Sustainable Agroecosystems, Department of Environmental Systems Science, ETH Zurich, Zurich, Switzerland

ABSTRACT

Increasing global temperatures have the potential to stimulate decomposition and alter the composition of soil organic matter (SOM). However, questions remain about the extent to which SOM quality and quantity along the soil profile may change under future warming. In this study we assessed how $+4\,°C$ whole-soil warming affected the quantity and quality of SOM down to 90 cm depth in a mixed-coniferous temperate forest using biomarker analyses. Our findings indicate that 4.5 years of soil warming led to divergent responses in subsoils (>20 cm) as compared to surface soils. Warming enhanced the accumulation of plant-derived *n*-alkanes over the whole soil profile. In the subsoil, this was at the expense of plant- and microorganism-derived fatty acids, and the relative abundance of SOM molecular components shifted from less microbially transformed to more transformed organic matter. Fine root mass declined by $24.0 \pm 7.5\%$ with warming over the whole soil profile, accompanied by reduced plant-derived inputs and accelerated decomposition of aromatic compounds and plant-derived fatty acids in the subsoils. Our study suggests that warming accelerated microbial decomposition of plant-derived inputs, leaving behind more degraded organic matter. The non-uniform, and depth dependent SOM composition and warming response implies that subsoil carbon cycling is as sensitive and complex as in surface soils.

1. Introduction

Climate warming is predicted to stimulate the decomposition of soil organic matter (SOM), potentially turning global soil into a source of greenhouse gases and thus generating positive feedbacks with future climate change (Davidson and Janssens, 2006; Hicks Pries et al., 2017; Melillo et al., 2017). However, the magnitude and rate of the decomposition response remains uncertain, as SOM decomposition is mediated by biogeochemical processes as well as substrate quality and availability that respond to warming on different timescales (Davidson and Janssens, 2006; Fontaine et al., 2007; Melillo et al., 2017). In addition, indirect effects of warming on nutrient cycling (Pendall et al., 2004) or plant inputs (Bradford et al., 2016; Müller et al., 2016) may have cascading effects on SOM quality and quantity (Lu et al., 2013) and consequently on microbial decomposition of SOM. Despite more than three decades of research, experimental evidence exploring linkages between warming and biogeochemical processes on SOM decomposition under field conditions is still limited.

Most soil warming experiments have focused on the response of surface SOM (ca. 20 cm depth) (van Gestel et al., 2018), and report accelerated microbial respiration under warming (Lu et al., 2013; Melillo et al., 2017). Yet, subsoil SOM which makes up 50% of global SOM (Jobbágy and Jackson, 2000; Rumpel et al., 2012) has rarely been examined, but has been assumed to be relatively stable and unresponsive to warming (Harrison et al., 2011). The Intergovernmental Panel on Climate Change (IPCC) models project an increase in subsoil temperatures by 4.5 °C globally by 2100 under RCP 8.5 scenario, nearly in synchrony with surface-soil and air temperatures (IPCC, 2019; Soong et al., 2020b). Rising soil temperatures may increase the decomposition of subsoil SOM, including recent plant-derived material (Hicks Pries et al., 2017) or old, previously stable pools (Vaughn and Torn, 2019). Subsoil microbial communities and microenvironment differ from those at the surface (Rumpel et al., 2012). Warming may change subsoil microbial community composition and functioning (Fontaine et al., 2007) as a result of altered plant inputs (Morrison et al., 2019). Thus, SOM, plant and microbial biomass responses to warming, especially in

---

subsoils, are key uncertainties in future predictions of the carbon cycle (Bradford et al., 2016).

Only recently whole soil warming experiments have delivered results showing that warming stimulates soil respiration in deep soil (Hicks Pries et al., 2017), although it has been difficult to quantify changes in SOM stocks (Jung et al., 2019; Li et al., 2019; Lu et al., 2013) due to large, pre-existing SOM stocks and its spatial heterogeneity. We could overcome the limitations of bulk observations by the use of molecular markers (such as solvent-extractable lipids) and SOM functional groups, which allow us to follow qualitative and quantitative alterations in composition, sources, and processes contributing to SOM dynamics (Jansen and Wiesenberg, 2017; Pisani et al., 2015).

In this study, we assessed how 4.5 years of soil warming ($+4\,^{\circ}$C) in a coniferous temperate forest changed the molecular composition and SOM degradation level at soil depths down to 90 cm, depths that spanned a range of decomposition conditions. Previous studies at the same experiment showed that warming increased soil respiration throughout the whole soil profile over the first 5 years of warming (Hicks Pries et al., 2017; Soong et al., 2021). With enhanced respiration, we anticipated a stronger decomposition of pre-existing SOM in the subsoils, where plant inputs are relatively few, compared to surface soils. To explore potential shifts in SOM composition in response to warming, we employed complementary molecular-level analyses which included: plant- and microorganism-derived compounds (alkanes and alkanoic acids) to investigate the fate and degradation of plant- and microorganism-derived organic matter in the soil and diffuse reflectance infrared Fourier transform (DRIFT) spectroscopy to investigate the quality of SOM. Molecular markers are determined on a small yet representative fraction of total SOM (Hedges et al., 2000). The investigated molecular markers carry information on sources and transformation processes, and reflect the behavior of SOM components of similar origins (Feng and Simpson, 2011; Kögel-Knabner, 2002). We also analyzed organic horizon (O-horizon) material and coarse and fine root mass throughout the profile to explore whether there were changes in plant-derived inputs that could affect the quality and quantity of SOM. Overall, we hypothesized that the depth-dependent change in plant inputs and decomposition processes would alter the quality and increase the level of degradation of SOM, especially in the subsoil.

2. Materials and methods

2.1. Study site and sampling

The whole-soil profile warming experiment is located at the University of California Blodgett experimental forest in the foothills of the Sierra Nevada, CA (120°39′40″W; 38°54′43″N; 1370 m a.s.l.). The site has a Mediterranean climate with a mean annual air temperature and precipitation of 12.5 °C and 1774 mm, respectively, with most of the precipitation occurring from November through April (Bird and Torn, 2006). The soil is an ultic Alfisol of granitic origin with fine-loam texture (mean pH of 5.5) and a developed O horizon of ca. 5 cm thickness (Rasmussen et al., 2005) and 16.6 ± 1 kg OC m^{-2} in the top meter (Hicks Pries et al., 2018). The experiment is situated in a thinned 80-year-old stand of mixed conifers, dominated by ponderosa pine (*Pinus ponderosa*), sugar pine (*Pinus lambertiana*), incense cedar (*Calodefrus decurrens*), white fir (*Abies concolor*), and douglas fir (*Pseudotsuga menziesii*) (Hicks Pries et al., 2017).

The soil warming experiment began in October 2013. The experimental design consists of six circular plots of 3 m diameter grouped into three replicated blocks each having a warmed and a control plot. The average soil temperature in the warmed plots was elevated by $+4\,^{\circ}$C to >1 m depth above the control plots ($+2.6\,^{\circ}$C warming at 0–20 cm depth), while maintaining the seasonality and natural temperature gradient with depth, with the use of buried resistance heater cable installed vertically inside 2.4 m long steel pipes (spaced 50 cm apart around the plot circumference) (Hanson et al., 2011). The setup of the control plots is identical to the warmed plots except heating was not turned on (Hicks Pries et al., 2017).

Two soil cores (diameter 4.78 cm) were collected using a manual auger from each of the six plots in April 2018 (after 4.5 years of warming). Soil samples from each plot were separated into O-horizon material (Oi, Oe, and Oa if they could be separated) and mineral soil into 10 cm increments from 0 to 90 cm depth. The soil samples were stored at 4 °C until being transported to the laboratory. A preliminary analysis of both cores for carbon and nitrogen concentrations showed <10% within-plot variability. For this manuscript, results from one soil core are presented.

2.2. Soil characteristics

In the laboratory, soil samples were freeze-dried to constant weight and passed through a 2 mm sieve to remove any stones, roots, or litter fragments. Roots that passed through the 2 mm sieve were additionally picked from the soil manually. The soil particles attached to the roots were removed by gently washing the roots with deionized water in a 500 μm sieve. The roots were then carefully separated into fine roots (<2 mm diameter) and coarse roots (2–5 mm diameter). The separated roots and organic layers were oven dried at 40 °C to constant weight. A subsample of the sieved soil, roots, and organic layer were ground using a ball mill (MM400, Retsch, Haan, Germany) and analyzed by an elemental analyzer-isotope ratio mass spectrometer (EA-IRMS; Flash 2000-HT Plus, linked by Conflo IV to Delta V Plus isotope ratio mass spectrometer, Thermo Fisher Scientific, Bremen, Germany) for concentrations of carbon and nitrogen (%C, %N), as well as stable carbon and nitrogen isotope composition (δ^{13}C, δ^{15}N). Calibration was carried out using caffeine (Merck, Germany), and a soil reference material originating from a Chernozem (Harsum, Germany). Two analytical replicates were measured for all samples.

2.3. Bulk soil organic matter composition using DRIFT spectroscopy

To characterize warming-induced changes in SOM composition, 6 mg of ground soil sample was examined by diffuse reflectance infrared Fourier transform spectroscopy (DRIFT). Mid-infrared spectra were recorded using a Bruker TENSOR 27 spectrometer (Billerica, Massachusetts, USA) from 4000 to 400 cm^{-1} (average of 16 scans per sample at 4 cm^{-1} resolution). Infrared absorption bands were represented by functional groups as follows: aliphatic C–H (2900 cm^{-1}), aromatic esters, carbonyl/carboxyl C=O (1735–1720 cm^{-1}), aromatic C=C (1660–1600 cm^{-1}, 1430–1380 cm^{-1}), lignin-like residues (1515–1500 cm^{-1}), phenolic/cellulose (1260–1210 cm^{-1}), and aromatic C–H (880, 805, 745 cm^{-1}) carbon (Artz et al., 2008; Chatterjee et al., 2012; Leifeld, 2006; Niemeyer et al., 1992). A summary of the absorption bands associated with different compound classes can be found in Fig. 6.

2.4. Solvent extractable lipid biomarker analysis

A range of lipid biomarkers (alkanoic acids and alkanes) were selected to examine changes in SOM quality, quantity and degradation level. Bulk soils (<2 mm; ~10–80 g) and O- horizon and root material (~0.1–2 g) were subjected to solvent extraction following the protocol by Wiesenberg and Gocke (2017). Lipids were extracted using soxhlet extraction with dichloromethane: methanol (93:7; v/v). The extracts were separated into a neutral-, fatty acid- and polar fraction by solid phase separation using Silica 60 + 5% KOH, 63–200 μm, (Macherey-Nagel, Düren, Germany). The *n*-alkanes were separated from the neutral fraction using column chromatography (activated SiO$_2$; 70–230 mesh, 100 Å) and spiked with deuterated tetracosane (D$_{50}$C$_{24}$) as an internal standard prior to gas chromatographic (GC) analysis. An aliquot of the fatty acid fraction (FA) was spiked with deuterated eicosanoic acid (D$_{39}$C$_{20}$) as an internal standard for quantification and derivatized to fatty acid methyl esters (FAMEs) using boron trifluoride:methanol
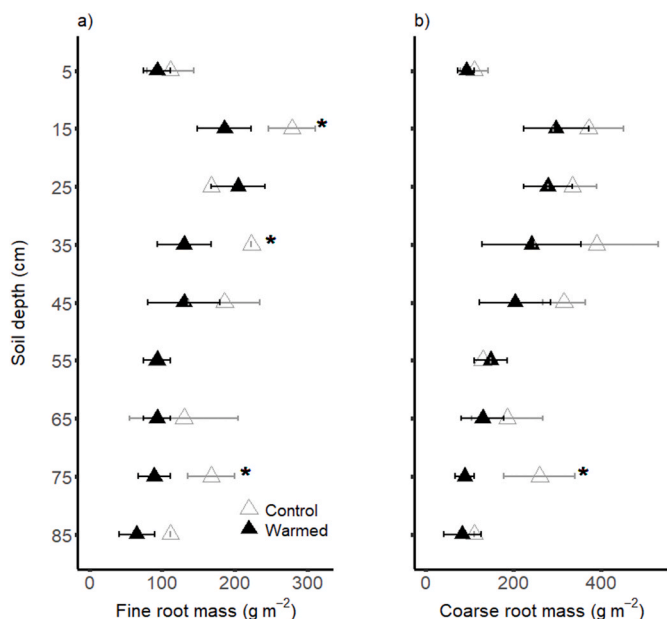
Fig. 1. a) Fine root mass (< 2 mm), b) Coarse root mass (2–5 mm) in the warmed and control plots (mean ± SE, n = 3) in 10 cm increments from 0 to 90 cm from the soil cores collected in April 2018. Significant treatment effects showing which depth increment changed with warming are indicated with asterisks: *p < 0.05.

solution (BF$_3$:MeOH) before GC analysis.

Individual compounds were quantified on an Agilent 7890B GC equipped with a multi-mode injector and a flame ionization detector using internal standards. Analytical errors were typically <5% based on

replicate analysis. Compound identification was performed on an Agilent 6890N GC equipped with split/splitless injector coupled to an Agilent 5973 mass selective detector (MS). Compound identification was done by comparison of mass spectra with those of external standards and from the NIST and Wiley mass spectra library. Both instruments were equipped with DB-5MS column (50 m × 0.2 mm x 0.33 μm) and 1.5 m de-activated pre-column, with helium as the carrier gas (1 ml min^{-1}). The GC oven temperature for *n*-alkanes was held at 70 °C for 4 min, and increased to 320 °C at a rate of 5 °C min^{-1} held for 50 min. For fatty acids (FA), the temperature was held at 50 °C for 4 min, then increased to 150 °C at a rate of 4 °C min^{-1}, and finally increased to 320 °C at 3 °C min^{-1} held for 40 min. On the GC-FID/MS, the samples (1 μl) were injected in splitless mode. The GC-MS was operated in electron ionization mode at 70 eV and scanned from m/z 50–550. The data acquired were processed with Chemstation software. The concentrations of the target compounds were normalized to the organic carbon concentrations of the respective sample (stated as μg g^{-1} OC).

Several molecular proxies have been applied to assess the source and degradation of organic matter in soils (Wiesenberg et al., 2010). Average chain length (ACL) is the weighted average of selected chain lengths of *n*-alkanes (C$_{23-35}$) and FA (C$_{14-32}$). Microbial-derived organic matter is characterized by shorter ACL than plant-derived organic matter, due to the absence of any long-chain FA (>C$_{19}$) and *n*-alkanes (>C$_{24}$) (Harwood and Russell, 1984). Therefore, ACL can be used as molecular proxy for the source and degradation of SOM (Wiesenberg et al., 2010). ACL was calculated as:

$$ACL = \sum (C_n * n) \bigg/ \sum C_n$$

where *n* is the number of carbons and C_n is the relative abundance of the respective compound with *n* carbons.

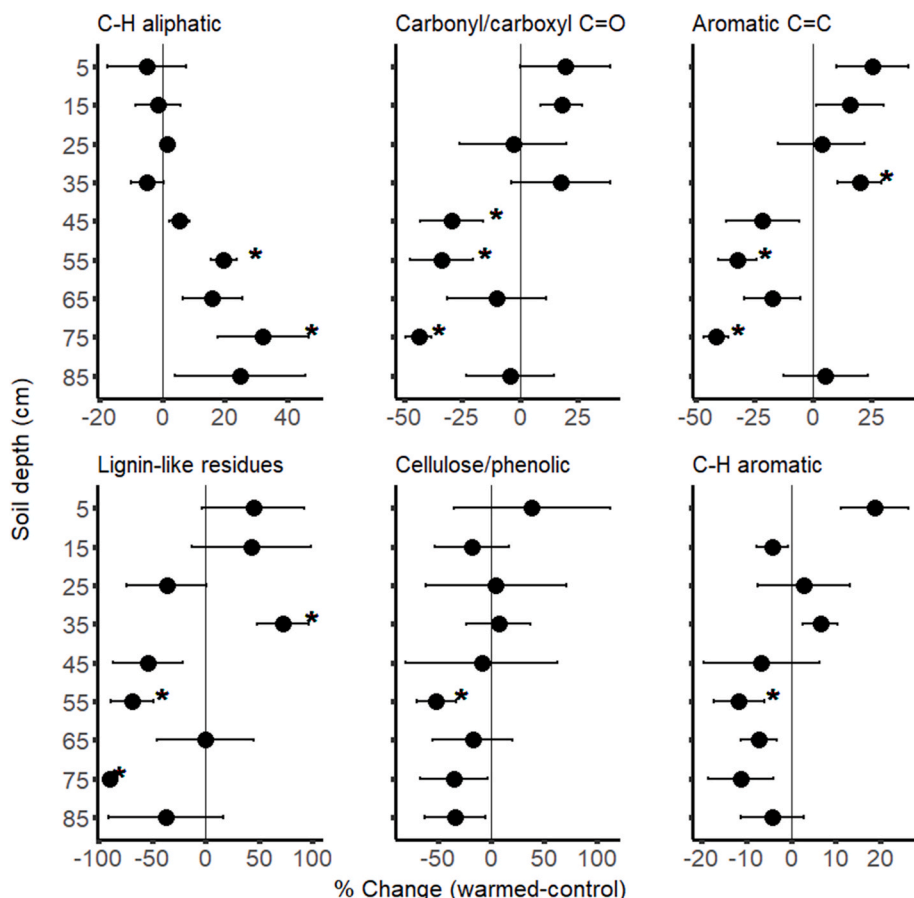Fresh plant-derived organic matter is characterized by odd-over-

Fig. 2. Warming-induced changes in the relative abundance of different functional groups identifiable by diffuse reflectance infrared Fourier transform (DRIFT) spectroscopy in warmed and control plots (mean ± SE, n = 3) expressed in % of change [(warmed-control)/control*100]. The spectral regions were assigned to C–H aliphatic, aromatic carbonyl/carboxyl C═O groups, aromatic C═C/ –COO$^-$ groups, lignin-like residues, cellulose/ phenolic, and C–H aromatics. A positive or negative value indicates that warming increased or reduced the relative abundance of the respective functional group. Significant treatment effects showing which depth increment changed with warming are indicated with asterisks: *p < 0.05.
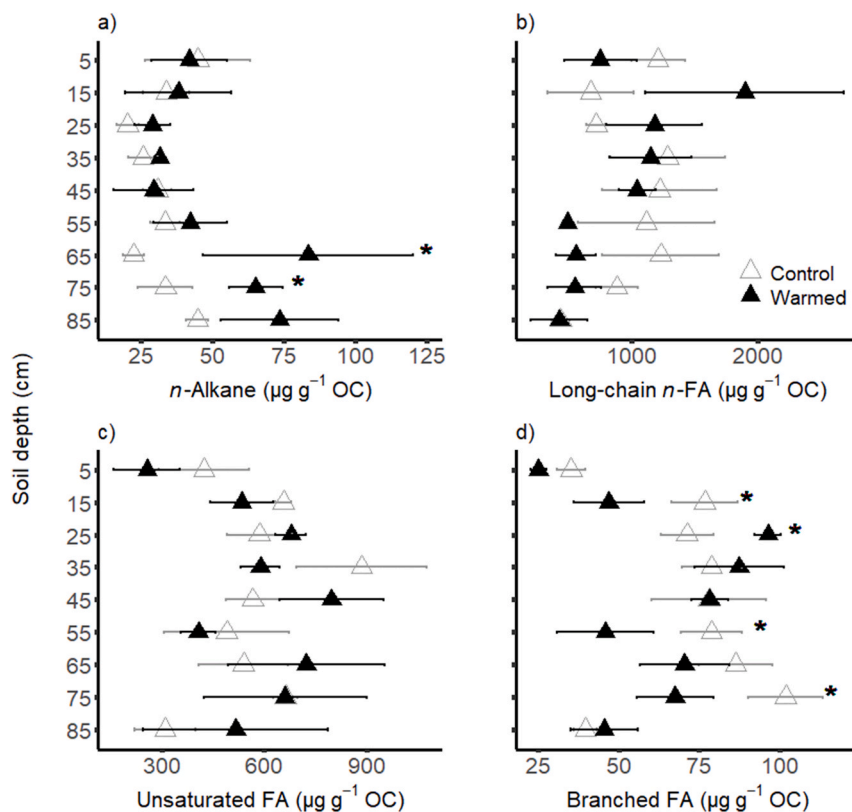
Fig. 3. Concentrations of solvent-extractable alkanes and fatty acids (FA) in the warmed and control plots in 10 cm increments from 0 to 90 cm (mean ± SE, n = 3): a) *n*-Alkanes (C_{23-35}), b) Long-chain *n*-fatty acids (C_{20-32}), c) Unsaturated fatty acids ($C_{16:1, \, 18:2, \, 18:1}$), d) Branched fatty acids (*iso*-C_{15}, *anteiso*-C_{15}, *iso*-C_{16}, *iso*-C_{17}, *anteiso*-C_{17}, *iso*-C_{19}). Significant treatment effects showing which depth increment changed with warming are indicated with asterisks: *$p < 0.05$.

even dominance for *n*-alkanes and even-over-odd dominance for *n*-fatty acids (Eglinton et al., 1962; Wiesenberg and Gocke, 2017). The carbon preference index (CPI) thus indicates input of mainly fresh plant-derived organic matter (high CPI > 10) or to which degree it has been degraded (values close to 1) (Angst et al., 2016; Cranwell, 1981). CPI was calculated as:

$$CPI_{FA} = \left[\left(\sum C_{20-30} \, even \Big/ \sum C_{19-29} \, odd \right) \right.$$
$$\left. + \left(\sum C_{20-30} \, even \Big/ \sum C_{21-31} \, odd \right) \right] \Big/ 2$$

$$CPI_{ALK} = \left[\left(\sum C_{23-35} \, odd \Big/ \sum C_{24-32} \, even \right) \right.$$
$$\left. + \left(\sum C_{23-35} \, odd \Big/ \sum C_{26-34} \, even \right) \right] \Big/ 2$$

for *n*-alkanes (CPI_{ALK}), and *n*-fatty acids (CPI_{FA}), respectively.

2.5. Statistical analyses

All data analysis was performed using the R v.3.6.3 (R Core Team, 2020) using the RStudio interface v. 1.2.5033 (RStudio Team, 2019). Roots, organic layers, and mineral soil samples were analyzed separately. Warming-induced changes in the relative abundance of individual functional groups was expressed as the % difference between warmed and control, normalized by the control value for each depth within each plot pair. Pairwise *t*-test was used to check whether the mean differences between warmed and control plots for each plot pair, or for each depth within each plot pair, was different from zero.

To test the effect of warming on lipid biomarkers, we built mixed effect models, using the functions *gls* and *lme* in the *nlme* package, using restricted maximum likelihood, with block (n = 3) as a random effect, and treatment, depth and their interaction as a fixed effect. In the model,

variance structures and autocorrelation were evaluated for inclusion based on corrected Akaike's Information Criterion (AIC). Autocorrelation was not included in our model as it did not improve the model fit. Normality and homoscedasticity in all models were visually checked using residuals and qqplots and adjusted when needed to meet model assumptions using log transformation. The level of significance was 5% ($p < 0.05$) in all statistical tests.

Principal component analysis (PCA) was performed using the function *prcomp* in the R *stats* package to investigate patterns in the SOM molecular composition generated by DRIFT spectra and lipid biomarker abundance. The PCA dataset included 54 data points with 10 variables. All variables were standardized before PCA analysis.

3. Results

3.1. Bulk SOM properties and composition

Fine root (<2 mm) mass in the control plots did not differ significantly with depth ($p = 0.055$; Fig. 1a), whereas coarse root (2–5 mm) mass decreased significantly with depth ($p = 0.022$; Fig. 1b). Overlaid on this pattern, warmed plots had 24.0 ± 7.5% less fine root mass than did the control plots averaged over all soil depths ($p = 0.017$), with markedly less fine root mass at 60–90 cm depth (−39.0 ± 5.4%; Fig. 1a). In addition, warmed plots had 25.9 ± 7.1% less coarse root mass than did the control plots for all soil depths ($p = 0.018$; Fig. 1b).

Soil organic carbon and nitrogen concentrations decreased with depth and were lower in the warmed plots below 20 cm ($p < 0.05$; Table 1). In contrast, there was a statistically non-significant increase in soil organic carbon and nitrogen concentrations in the top 20 cm ($p > 0.05$; Table 1). The C:N ratios did not differ between control and warmed plots when considering all soil depths or in the subsoil (below 20 cm) ($p > 0.05$; Table 1). The δ^{13}C values increased with depth and were similar
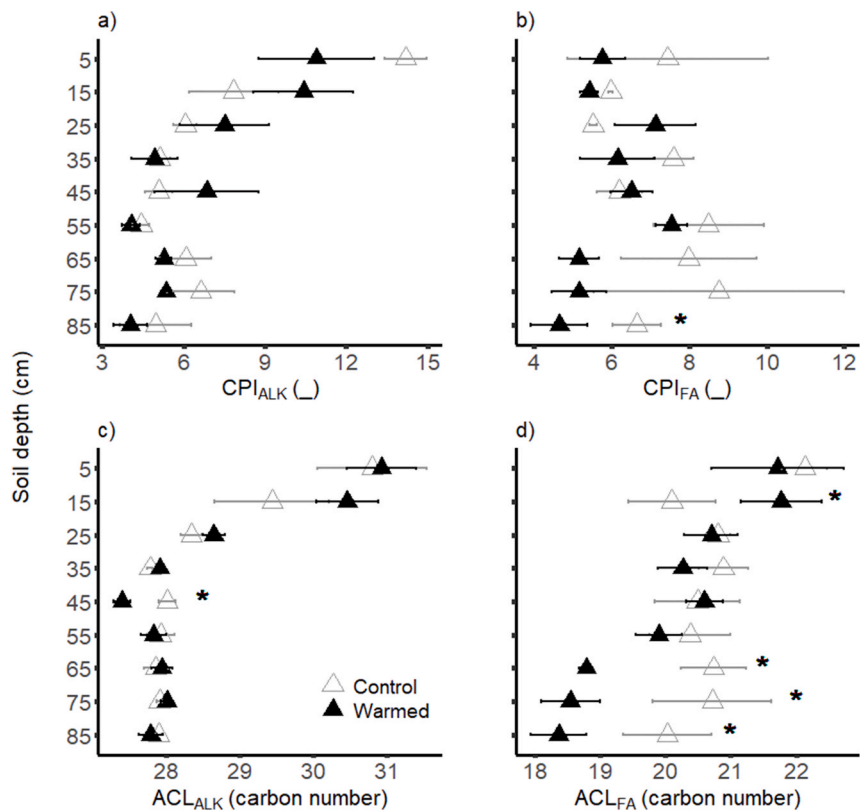
Fig. 4. Carbon preference index (CPI) of a) *n*-Alkanes (CPI$_{ALK}$) **and b)** Fatty acids (CPI$_{FA}$) **and average chain length (ACL) of c)** *n*-Alkanes (ACL$_{ALK}$) **and d)** Fatty acids (ACL$_{FA}$) in the warmed and control plots (mean ± SE, n = 3) in 10 cm increments from 0 to 90 cm. Significant treatment effects showing which depth increment changed with warming are indicated with asterisks: *$p < 0.05$.
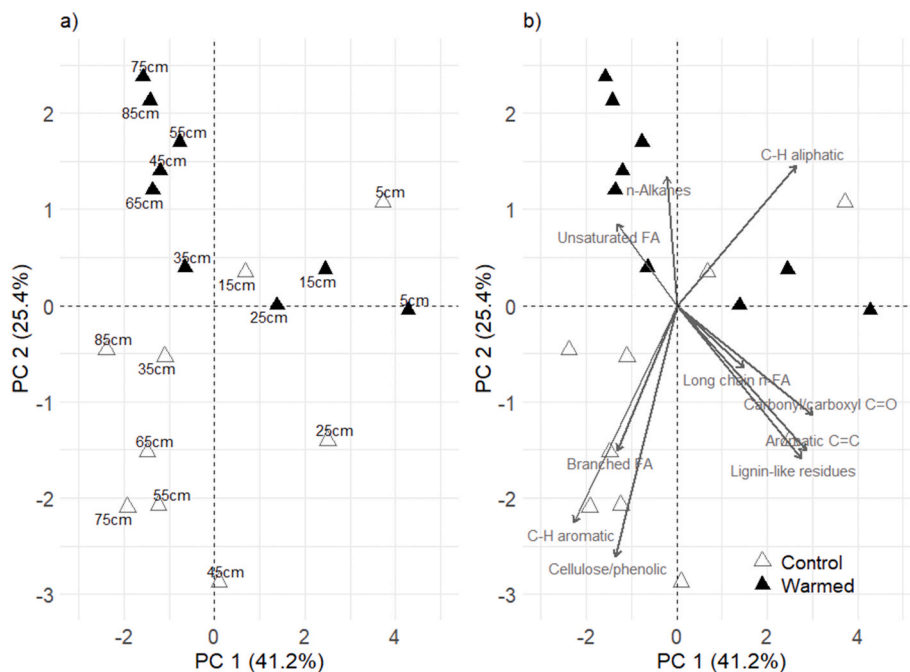

Fig. 5. Principal component analysis of biomarkers a) Individual soil depth and **b)** Biplots of soil depth and variables in the warmed and control plots (mean, n = 3) from 0 to 90 cm. The results are expressed as a biplot, where the distance and direction from the axis centre has the same meaning. Numbers in parenthesis represent data variations explained by the first two principal components (PC).

between control and warmed plots, except below 60 cm depth, where the values were 0.7 ± 0.1‰ higher in the warmed plots ($p = 0.005$; Table 1). A detailed description of carbon and nitrogen stocks from analysis of replicate cores can be found in Soong et al., (2021). Neither

δ^{13}C values nor soil organic carbon and nitrogen concentrations of the litter inputs (roots and O-horizon material) differed between control and warmed plots at any soil depth ($p > 0.05$; Table 1).

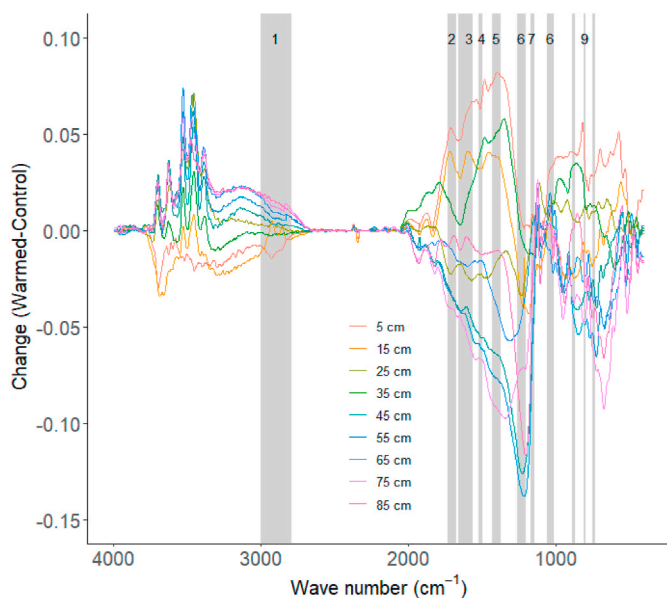Changes in SOM molecular composition with depth became apparent

Fig. 6. The absorption bands identifiable by diffuse reflectance infrared Fourier transform (DRIFT) spectroscopy (mean, n = 3) expressed as absolute change [warmed-control]. The regions marked in grey color were assigned to the following molecular vibrations for peak area integration: 1: 3000–2800 cm^{-1} aliphatic C–H, 2: 1735–1720 cm^{-1} aromatic esters, carbonyl/carboxyl C=O, 3: 1660–1600 cm^{-1} aromatic C=C/–COO−, 4: 1515–1500 cm^{-1} lignin-like residues, 5: 1430–1380 cm^{-1} aromatic C=C, 6: 1260–1210 cm^{-1} phenolic/cellulose, 7: 1170–1148 cm^{-1}, C–O bonds of poly-alcoholic and ether groups, 8: 1060–1020 cm^{-1} aliphatic C–O- and alcohol C–O, and 9: 880, 805, 745 cm^{-1} C–H aromatic. A positive or negative value indicates that warming increased or reduced the abundance of the respective functional group. (For interpretation of the references to color in this figure legend, the reader is referred to the Web version of this article.)

in diffuse reflectance infrared Fourier transform (DRIFT) spectra (Fig. 6). Warming altered the molecular chemistry of SOM, although not all depths responded in the same way. Warmed plots had $9.8 \pm 3.9\%$ more C–H aliphatic compounds than did the control plots averaged over all soil depths ($p = 0.017$; Fig. 2). In the surface soils (above 20 cm),

there was a statistically non-significant increase in the relative abundance of carbonyl/carboxyl C=O, and C=C aromatics compounds in the warmed plots relative to the control plots ($p > 0.05$; Fig. 6). However, in the subsoils (below 20 cm), warmed plots had $15.2 \pm 7.2\%$ and $11.9 \pm 5.7\%$ less carbonyl/carboxyl C=O ($p = 0.047$) and C=C aromatics ($p = 0.042$) respectively than did the control plots (Fig. 2). Furthermore, below 20 cm depth, warmed plots had less (non-significant) lignin-like residues ($30.5 \pm 20.1\%$; $p = 0.073$) and phenolic (cellulose) compounds ($19.7 \pm 14.9\%$; $p = 0.08$) relative to the control plots (Fig. 2).

3.2. Solvent-extractable lipid biomarkers

Changes in SOM quality and quantity were further investigated using lipid biomarker abundance. Plant-derived *n*-alkane (C$_{23–35}$) concentrations were more abundant in warmed plots relative to the control plots averaged over all soil depths ($p = 0.013$; Fig. 3a), with markedly more *n*-alkanes at 60–90 cm depth ($+45.7 \pm 13.6\%$; Fig. 3a). Neither long chain *n*-FA (C$_{20–32}$; Fig. 3b) nor unsaturated FA (C$_{16:1, \ 18:2 \ \& \ 18:1}$; Fig. 3c) concentrations in soils differed significantly ($p > 0.05$) between control and warmed plots averaged over all depths although warmed plots had $37.4 \pm 17.9\%$ less long chain *n*-FA concentrations than did the control plots below 60 cm ($p = 0.05$; Fig. 3b). In the litter inputs, *n*-alkane and long chain *n*-FA concentrations differed significantly between roots and O-horizon ($p < 0.05$; Table 2). The most prominent differences were observed in the *n*-alkanes which were less abundant in roots than in the O-horizon and soil (ca. −98%; Table 2). However, neither *n*-alkane nor long chain *n*-FA concentrations in roots and O-horizons differed significantly throughout the profile or in warmed plots relative to the control plots (Table 2). Microbially-derived branched FA (*iso*-C$_{15}$, *anteiso*-C$_{15}$, *iso*-C$_{16}$, *iso*-C$_{17}$, *anteiso*-C$_{17}$, *iso*-C$_{19}$) concentrations in soils increased significantly with depth ($p = 0.007$) in the control plots and were less abundant in warmed plots relative to the control plot ($-18.3 \pm 7.6\%$; $p = 0.031$; Fig. 3d).

Enhanced SOM degradation in the warmed plots was evidenced by SOM decomposition proxies, such as carbon preference index (CPI) and average chain length (ACL). With warming, both the *n*-alkanes proxies of CPI$_{ALK}$ and ACL$_{ALK}$ did not differ throughout the profile ($p = 0.335$ and $p = 0.556$ respectively) or in the subsoils (below 20 cm) of warmed plots compared to control plots (Fig. 4a; 4c). By contrast, warmed plots

Table 1
Soil organic carbon (SOC), and nitrogen (N) concentrations, δ^{13}C, and C:N ratio from the O-horizon, root material (fine and coarse roots) and soil (0–90 cm) in the warmed and control plots (mean ± SE, n = 3) from the soil core collected in April 2018, 4.5 years after the onset of soil warming. Significant treatment effects showing which depth increment changed with warming are indicated with asterisks: *$p < 0.05$.

		SOC (mg g^{-1} soil)		N (mg g^{-1} soil)		δ^{13}C (‰ VPDB)		C:N ratio	
		Control	Warmed	Control	Warmed	Control	Warmed	Control	Warmed
	Layer								
O-horizon	Oi	473.3 ± 5.2	481.0 ± 0.4	5.9 ± 0.6	5.9 ± 0.7	−27.1 ± 0.2	−28.6 ± 0.7	82.4 ± 9.9	83.8 ± 9.2
	Oe	429.5 ± 14.3	418.6 ± 44.8	8.4 ± 1.0	7.3 ± 0.3	−26.8 ± 0.3	−26.8 ± 0.0	52.7 ± 7.8	57.4 ± 7.0
	Oa	367.0	230.5 ± 99.1	4.8	6.1 ± 2.4	−24.9	−26.3 ± 0.1	77.1	36.8 ± 2.0
	Depth								
Roots	0–30 cm	442.9 ± 10.6	433.3 ± 17.3	4.6 ± 0.6	4.3 ± 0.8	−27.2 ± 0.3	−27.3 ± 0.1	98.2 ± 12.2	104.9 ± 14.7
	30–60 cm	450.0 ± 12.4	462.4 ± 14.3	3.3 ± 0.4	4.2 ± 1.1	−27.4 ± 0.3	−26.6 ± 0.3	141.5 ± 17.9	121.5 ± 23.8
	60–90 cm	450.4 ± 14.5	486.7 ± 36.2	3.1 ± 0.4	3.0 ± 0.3	−27.2 ± 0.4	−27.1 ± 0.4	153.2 ± 19.1	166.4 ± 23.1
Mineral soil	0–10 cm	71.3 ± 10.9	60.4 ± 6.7	2.3 ± 0.4	3.0 ± 0.8	−25.7 ± 0.8	−25.5 ± 0.5	32.3 ± 3.5	28.6 ± 2.4
	10–20 cm	32.5 ± 8.6	53.2 ± 18.6	1.3 ± 0.3	1.4 ± 0.3	−24.8 ± 0.3	−25.0 ± 0.6	25.1 ± 2.1	28.0 ± 3.5
	20–30 cm	23.3 ± 7.8	14.5 ± 3.1	0.8 ± 0.3	0.6 ± 0.1	−24.7 ± 0.1	−24.8 ± 0.2	28.9 ± 2.8	26.3 ± 2.6
	30–40 cm	13.2 ± 3.9	7.1 ± 1.3	0.5 ± 0.1	0.3 ± 0.1	−24.9 ± 0.2	−24.4 ± 0.4	27.6 ± 4.4	25.8 ± 3.3
	40–50 cm	7.5 ± 1.5	6.1 ± 0.4	0.3 ± 0.1	0.3 ± 0.0	−24.5 ± 0.1	−24.4 ± 0.3	24.0 ± 0.1	23.9 ± 2.1
	50–60 cm	4.6 ± 1.1	3.6 ± 1.0	0.2 ± 0.1	0.2 ± 0.0	−24.0 ± 0.2	−24.0 ± 0.1	23.3 ± 1.4	22.8 ± 4.9
	60–70 cm	5.0 ± 0.2	2.5 ± 0.4*	0.2 ± 0.0	0.1 ± 0.0*	−24.4 ± 0.4	−23.6 ± 0.1*	28.2 ± 3.9	22.8 ± 3.0
	70–80 cm	6.8 ± 3.4	2.3 ± 0.2*	0.2 ± 0.1	0.1 ± 0.0	−24.5 ± 0.4	−23.6 ± 0.3*	28.9 ± 5.8	22.3 ± 4.3
	80–90 cm	3.1 ± 0.8	2.1 ± 0.1	0.1 ± 0.0	0.1 ± 0.0	−24.2 ± 0.1	−23.7 ± 0.2	27.2 ± 0.8	22.4 ± 0.6*

For the Oa layer (O-horizon) in the control plot, n = 1. Significant treatment effects are indicated with asterisks: *p < 0.05.

Table 2
Concentrations of **n-Alkanes and long-chain n-fatty acids**, and carbon preference index (CPI) of **n-Alkanes (CPI$_{ALK}$)** and fatty acids (CPI$_{FA}$) and average chain length (ACL) of **n-Alkanes (ACL$_{ALK}$) and fatty acids (ACL$_{FA}$)** from the O-horizon, and root material (fine and coarse roots) in the warmed and control plots (mean ± SE, n = 3).

		n-Alkanes (μg g^{-1} OC)		Long-chain n-FA (μg g^{-1} OC)		CPI$_{FA}$		ACL$_{FA}$		CPI$_{ALK}$		ACL$_{ALK}$	
		Control	Warmed	Control	Warmed	Control	Warmed	Control	Warmed	Control	Warmed	Control	Warmed
	Layer												
O-horizon	Oi	31.5 ± 3.6	27.3 ± 0.2	1950.2 ± 97.1	1876.0 ± 69.2	7.4 ± 1.2	8.8 ± 1.2	20.2 ± 0.6	21.0 ± 0.3	6.2 ± 1.1	6.1 ± 0.5	29.5 ± 0.5	28.7 ± 0.3
	Oe	90.0 ± 28.1	75.5 ± 17.6	1820.2 ± 83.6	1679.4 ± 31.9	9.7 ± 2.0	9.7 ± 1.0	22.1 ± 0.2	22.2 ± 0.2	16.5 ± 2.8	15.9 ± 0.5	31.9 ± 0.6	32.0 ± 0.2
	Oa	42.3	52.7 ± 37.3	686.0	1380.4 ± 81.9	9.8	9.4 ± 0.8	22.5	21.8 ± 0.5	15.2	19.5 ± 1.2	32.4	32.4 ± 0.2
	Depth												
Roots	0–30 cm	0.4 ± 0.2	0.1 ± 0.1	1092.0 ± 80.3	2860.2 ± 67.5	9.6 ± 2.2	12.4 ± 6.8	20.9 ± 0.4	21.1 ± 0.6	nd	nd	nd	nd
	30–60 cm	nd	0.3 ± 0.1	2067.0 ± 12.7	2051.0 ± 0.7	10.3 ± 4.0	8.7 ± 5.5	21.2 ± 0.2	21.2 ± 0.4	nd	nd	nd	nd
	60–90 cm	0.2 ± 0.2	nd	2837.2 ± 82.9	2411.9 ± 9.1	5.7 ± 0.2	7.9 ± 3.9	21.4 ± 0.1	20.6 ± 0.4	nd	nd	nd	nd

For the Oa layer (O horizon) in the control plot, n = 1; nd = not quantifiable.

had lower carbon preference index values of FA (CPI$_{FA}$; mostly < 6) relative to the control plots averaged over all soil depths ($p = 0.041$), with pronounced differences below 60 cm depth ($p = 0.018$, warming × depth interaction, $p = 0.059$; Fig. 4b). The average chain length of FA (ACL$_{FA}$) was significantly shorter in the warmed plots than in the control plots ($p = 0.036$), and more pronounced below 50 cm (warming × depth interaction, $p = 0.038$; Fig. 4d). Notably, CPI$_{FA}$ and ACL$_{FA}$ values observed in soils in the control plots were similar to those observed in roots and the O-horizon (Fig. 4b; 4d; Table 2). Both the CPI$_{FA}$ and ACL$_{FA}$ of roots and the O-horizons did not differ significantly between different depths or in warmed plots relative to the control plots (Table 2).

3.3. Principle component analysis

Finally, changes in SOM molecular profiles were explored using PCA in the warmed and control plots. The first two principle components (PC) explained 66.6% of the variation of the data (PC 1 = 41.2% and PC 2 = 25.4%; Fig. 5). PC 1 separated n-alkanes, unsaturated FA, branched FA, C–H aromatics and phenolic/cellulose compounds (negative contribution) from long chain n-FA, C–H aliphatics, carbonyl/carboxyl C=O, C=C aromatics and lignin-like residues (positive contribution). PC 2 separated n-alkane, unsaturated FA and C–H aliphatic (positive contribution) from long chain n-FA, branched FA, C–H aromatics, phenolic/cellulose compounds, carbonyl/carboxyl C=O, C=C aromatics and lignin-like residues (negative contribution) (Fig. 5b).

The surface soil (0–20 cm) samples did not cluster according to treatment but were separated from subsoils along PC1 (Fig. 5a). Subsoils (below 30 cm) were grouped mainly by treatment along PC2 with warmed plots being clearly separated from the control plots (Fig. 5a). These results show an accumulation of aliphatic components of SOM at the expense of aromatic compounds and plant- and microorganism-derived fatty acids in the warmed subsoil.

4. Discussion

Four and a half years of whole-soil experimental warming in a coniferous temperate forest significantly altered the quality and quantity of SOM. The combined use of complementary biogeochemical analyses revealed marked reduction in plant root densities and accelerated decomposition of SOM. Majority of these changes were more pronounced in the subsoils (below 20 cm), highlighting the sensitivity of subsoil carbon to increasing global temperatures.

4.1. Bulk SOM characteristics change along the soil profile with warming

Experimental warming led to divergent responses in different SOM molecular components across soil depths. While warming enhanced the accumulation of n-alkanes (Fig. 3a) and aliphatic functional groups (Fig. 2) over the whole soil profile, degradation of plant- and microorganism-derived fatty acids (Fig. 3b; 3d) and aromatic compounds (Fig. 2) was only enhanced in the subsoils (below 20 cm depth). The observed accumulation of n-alkanes with warming over the whole soil profile is consistent with previous observations of selective accumulation of aliphatic carbon with short-term soil warming in both surface soils (Feng et al., 2008; Li et al., 2019; Pisani et al., 2015) and subsoils (Jia et al., 2019) in grassland and forest ecosystems. Furthermore, warmed subsoils showed signatures of increased microbial processing of plant-derived inputs such as an enrichment in δ^{13}C (Table 1) of the remaining organic matter (Ehleringer et al., 2000).

Collectively, the above changes suggest that subsoil SOM is more sensitive to warming than is surface soil SOM in this coniferous forest site. The observed differences in SOM quality and quantity in the subsoil vs surface soil can be attributed to changes in the rate of plant inputs (Morrison et al., 2019) and/or in microbial abundance and activity (Fontaine et al., 2007), and to contrasting physicochemical conditions with depth (Hicks Pries et al., 2017; Vaughn and Torn, 2019).

Multivariate analysis helps to further corroborate our finding that there is a distinct response between surface- and subsoil SOM to warming (Fig. 5). Whereas surface SOM is dominated by recent (less transformed) plant-litter inputs, subsoil SOM is relatively more degraded and transformed than that close to the surface. The lack of change in plant- and microorganism-derived organic matter in the surface soil may be due to slight drying at the surface in summer, and lower level of warming near the surface (+2.6 °C) (Soong et al., 2021) which could have inhibited or resulted in relatively less enhancement of microbial decomposition of SOM, and/or to increased surface inputs; we note that the aboveground trees were not warmed.

4.2. Molecular markers reflect reduced root input with warming

The importance of root dynamics in regulating ecosystem carbon cycling is recognized (e.g., Parts et al., 2019; Song et al., 2019). Changes in root inputs can affect SOM quantity and composition since roots are an important source of deep soil carbon (Rasse et al., 2005; Sokol et al., 2018). For instance, changes in root-derived inputs (including exudates) can drive changes in the composition of the soil microbial community (Huo et al., 2017) and may result in different rates of microbial decomposition at different depths. In our experiment, both fine and coarse root mass (living and dead; Fig. 1) were reduced with warming, suggesting a loss of SOM or that warming accelerated root decomposition. The observed decline in root mass with warming (Fig. 1) could have been responsible for the decrease in SOM (Table 1; Soong et al., 2021). In mesic forests, root growth is regulated by soil water and nutrient availability (Bai et al., 2010; Parts et al., 2019). Increased temperatures can cause depletion in soil water resulting in increased fine root mortality (Parts et al., 2019; Wan et al., 2004). In our experiment, warming resulted in 2–5% (percentage points) decrease in the volumetric water content throughout the profile (Soong et al., 2021). This moisture depletion could help explain the observed decrease in root mass (Parts et al., 2019). Previous studies showed a range of responses in root biomass of surface soils to warming, either an increase (Keuper et al., 2017; Li et al., 2019; Lim et al., 2018), a decrease (Arndal et al., 2018; Bai et al., 2010; Parts et al., 2019; Solly et al., 2017; Wan et al., 2004), or no change (Johnson et al., 2006; Jung et al., 2019; Wang et al., 2017) in grassland and forest ecosystems. The observed decrease in both fine and coarse root mass with warming over the whole soil profile adds a new dimension to previous observations that root biomass decreases in surface soils exposed to warming (e.g. Arndal et al., 2018; Parts et al., 2019) and contradicts other studies that showed no or positive change (e.g. Jung et al., 2019; Li et al., 2019).

In our experiment, warming altered SOM molecular composition at all soil depths, with the largest differences below 20 cm depth. This result was likely caused by a combination of a decrease in root-derived inputs (Parts et al., 2019; Wan et al., 2004), preferential loss or transformation of SOM compounds (Jia et al., 2019), and warming-induced shifts in microbial activity (Clemmensen et al., 2006; Morrison et al., 2019; Pold et al., 2017; Rillig et al., 2002), based on several lines of evidence. First, the observed decline in root input is likely to be responsible for the lower concentrations of plant-derived FA (Fig. 3b), since roots were enriched in FA compared to O-horizons (aboveground input) (Table 2). Second, the enhanced accumulation of *n*-alkanes (Fig. 3a), possibly stemming from degradation products of other aliphatic compounds (i.e. long chain *n*-FA) (Otto and Simpson, 2005) and consistent with the reduced concentrations of plant-derived long chain *n*-FA and branched FA (Fig. 3b; 3d), suggests preferential loss or transformation of SOM compounds. Notably, CPI$_{ALK}$ and ACL$_{ALK}$ proxies (Fig. 4a; 4c) did not differ between warmed and control plots, and were similar to those observed in the O-horizon (Table 2), suggesting similar input of fresh OM (Gocke et al., 2014). Possibly the source of *n*-alkanes could be microbial-derived carbon, as indicated by decreasing degradation proxies in the warmed subsoils (CPI$_{FA}$ and ACL$_{FA}$; Fig. 4b; 4d). Third, branched alkanoic acids (*iso*-C$_{15}$, *anteiso*-C$_{15}$, *iso*-C$_{16}$, *iso*-C$_{17}$,

anteiso-C$_{17}$, *iso*-C$_{19}$) (Fig. 3d), which are mainly biosynthesized by bacteria and fungi (Otto and Simpson, 2005), declined with warming suggesting lower abundances of bacterial and fungal microbial communities. Further investigation of the microbial responses to warming is needed to resolve the cause of the molecular responses found here.

4.3. Warming increases the degree of SOM decomposition at depth

Solvent-extractable short chain lipids have been considered to be easily decomposable components of SOM (Pisani et al., 2015), whereas aliphatic and aromatic compounds are believed to be degraded more slowly (Hedges et al., 1988; Marschner et al., 2008; Riederer et al., 1993; Rumpel et al., 2002). This concept of intrinsic degradability has been questioned (Lehmann and Kleber, 2015). In fact, we observed that the effect of warming did not follow these categories in a simple way. We observed shifts in both easily degradable plant- and microorganism-derived fatty acids and in more slowly degradable aromatic compounds (Fig. 2; 3; 5). This uniform degradation pattern confirms observations from a grassland warming experiment (Jia et al., 2019) but contrasts with other studies that found a decrease in compounds considered to be labile (e.g. Pold et al., 2017) or compounds considered recalcitrant (e.g. Li et al., 2019; Pisani et al., 2015), but not both. Studies from forest and alpine ecosystems did not find similar patterns as observed in our experiment (Schnecker et al., 2016; Zhao et al., 2018). Thus, there is no simple relationship between relative molecular complexity and effect of warming.

We hypothesize that with warming the combination of decreasing organic matter inputs from root litter and accelerated microbial decomposition might cause faster decomposition of both easily degradable plant- and microorganism-derived fatty acids and slower degradable aromatic compounds based on several lines of evidence. First, *n*-alkanes, which increased (Fig. 3a), stem from the degradation of fatty acids, ketones, alcohols and biopolymers such as cutin and suberin (Otto and Simpson, 2005). In this experiment, dissolved organic carbon concentrations increased with warming (Soong et al., 2021), potentially alleviating carbon limitation in subsoils (Soong et al., 2020a), and subsequently fueling decomposition of easily and slowly degradable compounds. Second, the degradation proxies (CPI$_{FA}$, and ACL$_{FA}$; Fig. 4b and d) suggest that in the warmed subsoils (>50 cm) we find more microbial processed carbon at the expense of plant-derived SOM. Indeed, Soong et al., 2021 observed a loss in soil organic carbon stocks below 20 cm in this experiment, primarily from plant and particulate matter and attributed these changes to enhanced SOM decomposition with warming. Our results support that hypothesis, and suggest a decrease in root-derived inputs and/or enhanced decomposition of young, fresh plant-derived SOM. Third, we also observed indications for more advanced stages of microbial degradation of plant-derived organic matter such as an enrichment in δ^{13}C (Table 1) of the remaining organic matter (Ehleringer et al., 2000). Taken together, our results suggest enhanced decomposition of both easily and slowly degradable organic compounds with warming, leading to a shift in overall SOM composition from plant-derived to microbial-derived and transformed material. Our results are consistent with previous observations of enhanced decomposition of complex organic matter such as lignin in surface soils (0–20 cm) (Li et al., 2019; Pold et al., 2015) and subsoils (20–50 cm) (Jia et al., 2019) exposed to warming. However, it is important to complement our results with long-term, time-resolved analysis including from other ecosystems to test if the findings are generalizable, and to improve confidence in future projections of SOM dynamics.

5. Conclusion

Four and a half years of whole-soil experimental warming altered the quality and quantity of SOM. Warming led to preferential loss of plant-derived organic matter and altered the molecular composition of SOM

from less microbially transformed to more transformed organic matter, mainly in the subsoil. Both fine and coarse root mass declined with warming, accompanied by reduced plant-derived inputs and accelerated decomposition of aromatic compounds and accumulation of plant-derived *n*-alkanes at the expense of plant- and microorganism-derived fatty acids in the subsoils. Taken together, our results suggest that not only easily degradable plant- and microorganism-derived OM, but also slowly degradable aromatic compounds are more sensitive to warming in the subsoil compared with surface soil. Warming led to a loss of young, fresh easily accessible organic matter, leaving behind relatively more degraded and possibly more stable SOM. This loss of plant-derived SOM could affect soil functions, for example related to agriculture and hydrology, and eventually might reduce total soil carbon storage potential in a warmer climate.

Author contributions

MST designed and maintained the warming field experiment. MS conceived the DEEP C project. All co-authors participated in the field campaign, data interpretation, and contributed actively to the manuscript written by NO. NO carried out biogeochemical analyses, supervised by GW, and ES analyzed root mass.

Author information

The authors declare no competing interests. Correspondence and requests for materials should be addressed to: nicholas.ofiti@geo.uzh.ch.

Data availability

The data used in this study will be available on the ESS-DIVE repository (https://ess-dive.lbl.gov/) upon acceptance.

Declaration of competing interest

The authors declare that they have no known competing financial interests or personal relationships that could have appeared to influence the work reported in this paper.

Acknowledgments

Appendix A. Supplementary data

Supplementary data to this article can be found online at https://doi.org/10.1016/j.soilbio.2021.108185.

References

Angst, G., John, S., Müeller, C.W., Kögel-Knabner, I., Rethemeyer, J., 2016. Tracing the sources and spatial distribution of organic carbon in subsoils using a multi-biomarker approach. Scientific Reports 6.

Arndal, M.F., Tolver, A., Larsen, K.S., Beier, C., Schmidt, I.K., 2018. Fine root growth and vertical distribution in response to elevated CO₂, warming and drought in a mixed heathland–grassland. Ecosystems 21, 15–30.

Artz, R.R.E., Chapman, S.J., Jean Robertson, A.H., Potts, J.M., Laggoun-Défarge, F., Gogo, S., Comont, L., Disnar, J.R., Francez, A.J., 2008. FTIR spectroscopy can be used as a screening tool for organic matter quality in regenerating cutover peatlands. Soil Biology and Biochemistry 40, 515–527.

Bai, W., Wan, S., Niu, S., Liu, W., Chen, Q., Wang, Q., Zhang, W., Han, X., Li, L., 2010. Increased temperature and precipitation interact to affect root production, mortality, and turnover in a temperate steppe: implications for ecosystem C cycling. Global Change Biology 16, 1306–1316.

Bird, J.A., Torn, M.S., 2006. Fine roots vs. needles: a comparison of ¹³C and ¹⁵N dynamics in a Ponderosa pine forest soil. Biogeochemistry 79, 361–382.

Bradford, M.A., Wieder, W.R., Bonan, G.B., Fierer, N., Raymond, P.A., Crowther, T.W., 2016. Managing uncertainty in soil carbon feedbacks to climate change. Nature Climate Change 6, 751.

Chatterjee, S., Santos, F., Abiven, S., Itin, B., Stark, R.E., Bird, J.A., 2012. Elucidating the chemical structure of pyrogenic organic matter by combining magnetic resonance, mid-infrared spectroscopy and mass spectrometry. Organic Geochemistry 51, 35–44.

Clemmensen, K.E., Michelsen, A., Jonasson, S., Shaver, G.R., 2006. Increased ectomycorrhizal fungal abundance after long-term fertilization and warming of two arctic tundra ecosystems. New Phytologist 171, 391–404.

Cranwell, P.A., 1981. Diagenesis of free and bound lipids in terrestrial detritus deposited in a lacustrine sediment. Organic Geochemistry 3, 79–89.

Davidson, E.A., Janssens, I.A., 2006. Temperature sensitivity of soil carbon decomposition and feedbacks to climate change. Nature 440, 165–173.

Eglinton, G., Gonzalez, A.G., Hamilton, R.J., Raphael, R.A., 1962. Hydrocarbon constituents of the wax coatings of plant leaves: a taxonomic survey. Phytochemistry 1, 89–102.

Ehleringer, J.R., Buchmann, N., Flanagan, L.B., 2000. Carbon isotope ratios in belowground carbon cycle processes. Ecological Applications 10, 412–422.

Feng, X., Simpson, M.J., 2011. Molecular-level methods for monitoring soil organic matter responses to global climate change. Journal of Environmental Monitoring 13 (5), 1246–1254. https://doi.org/10.1039/c0em00752h.

Feng, X.J., Simpson, A.J., Wilson, K.P., Williams, D.D., Simpson, M.J., 2008. Increased cuticular carbon sequestration and lignin oxidation in response to soil warming. Nature Geoscience 1, 836–839.

Fontaine, S., Barot, S., Barré, P., Bdioui, N., Mary, B., Rumpel, C., 2007. Stability of organic carbon in deep soil layers controlled by fresh carbon supply. Nature 450, 277–280.

Gocke, M., Peth, S., Wiesenberg, G.L.B., 2014. Lateral and depth variation of loess organic matter overprint related to rhizoliths - revealed by lipid molecular proxies and X-ray tomography. Catena 112, 72–85.

Hanson, P.J., Childs, K.W., Wullschleger, S.D., Riggs, J.S., Thomas, W.K., Todd, D.E., Warren, J.M., 2011. A method for experimental heating of intact soil profiles for application to climate change experiments. Global Change Biology 17, 1083–1096.

Harrison, R.B., Footen, P.W., Strahm, B.D., 2011. Deep soil horizons: contribution and importance to soil carbon pools and in assessing whole-ecosystem response to management and global change. Forest Science 57, 67–76.

Harwood, L.J., Russell, J.N., 1984. Lipids in Plants and Microbes.

Hedges, J.I., Blanchette, R.A., Weliky, K., Devol, A.H., 1988. Effects of fungal degradation on the CuO oxidation products of lignin: a controlled laboratory study. Geochimica et Cosmochimica Acta 52, 2717–2726.

Hedges, J.I., Eglinton, G., Hatcher, P.G., Kirchman, D.L., Arnosti, C., Derenne, S., Evershed, R.P., Kögel-Knabner, I., De Leeuw, J.W., Littke, R., Michaelis, W., Rullkötter, J., 2000. The molecularly-uncharacterized component of nonliving organic matter in natural environments. Organic Geochemistry 31, 945–958.

Hicks Pries, C.E., Castanha, C., Porras, R.C., Torn, M.S., 2017. The whole-soil carbon flux in response to warming. Science 355, 1420–1423.

Hicks Pries, C.E., Sulman, B.N., West, C., O'Neill, C., Poppleton, E., Porras, R.C., Castanha, C., Zhu, B., Wiedemeier, D.B., Torn, M.S., 2018. Root litter decomposition slows with soil depth. Soil Biology and Biochemistry 125, 103–114.

Huo, C., Luo, Y., Cheng, W., 2017. Rhizosphere priming effect: a meta-analysis. Soil Biology and Biochemistry 111, 78–84. https://doi.org/10.1016/j.soilbio.2017.04.003.

IPCC, 2019. Climate Change 2019 – Climate Change and Land: an IPCC Special Report on Climate Change, Desertification, Land Degradation, Sustainable Land Management, Food Security, and Greenhouse Gas Fluxes in Terrestrial Ecosystems.

Jansen, B., Wiesenberg, G.L.B., 2017. Opportunities and limitations related to the application of plant-derived lipid molecular proxies in soil science. Soils 3, 211–234.

Jia, J., Cao, Z., Liu, C., Zhang, Z., Lin, L., Wang, Y., Haghipour, N., Wacker, L., Bao, H., Dittmar, T., Simpson, M.J., Yang, H., Crowther, T.W., Eglinton, T.I., He, J., Feng, X., 2019. Climate warming alters subsoil but not topsoil carbon dynamics in alpine grassland. Global Change Biology gcb 14823.

Jobbágy, E., Jackson, R., 2000. The Vertical Distribution of Soil Organic Carbon and its Relation to Climate and Vegetation. Ecological Applications.

Johnson, M.G., Rygiewicz, P.T., Tingey, D.T., Phillips, D.L., 2006. Elevated CO₂ and elevated temperature have no effect on Douglas-fir fine-root dynamics in nitrogen-poor soil. New Phytologist 170, 345–356.

Jung, J.Y., Michelsen, A., Kim, M., Nam, S., Schmidt, N.M., Jung, S., Choe, Y.H., Lee, B.Y., Yoon, H.I., Lee, Y.K., 2019. Responses of surface SOC to long-term experimental warming vary between different heath types in the High Arctic tundra. European Journal of Soil Science 71, 752–767. https://doi.org/10.1111/ejss.12896.

Keuper, F., Dorrepaal, E., van Bodegom, P.M., van Logtestijn, R., Venhuizen, G., van Hal, J., Aerts, R., 2017. Experimentally increased nutrient availability at the permafrost thaw front selectively enhances biomass production of deep-rooting subarctic peatland species. Global Change Biology 23, 4257–4266.

Kögel-Knabner, I., 2002. The macromolecular organic composition of Plant and microbial residues as inputs to soil organic matter. Soil Biology and Biochemistry 34 (2), 139–162.

Lehmann, J., Kleber, M., 2015. The contentious nature of soil organic matter. Nature 528, 60.

Leifeld, J., 2006. Application of diffuse reflectance FT-IR spectroscopy and partial least-squares regression to predict NMR properties of soil organic matter. European Journal of Soil Science 57, 846–857.

Li, F., Peng, Y., Chen, L., Yang, G., Abbott, B.W., Zhang, D., Fang, K., Wang, G., Wang, J., Yu, J., Liu, L., Zhang, Q., Chen, K., Mohammat, A., Yang, Y., 2019. Warming alters surface soil organic matter composition despite unchanged carbon stocks in a Tibetan permafrost ecosystem. Functional Ecology 34, 911–922. https://doi.org/10.1111/1365-2435.13489.

Lim, H., Oren, R., Näsholm, T., Strömgren, M., Lundmark, T., Grip, H., Linder, S., 2018. Boreal forest biomass accumulation is not increased by two decades of soil warming. Nature Climate Change 9, 49–52.

Lu, M., Zhou, X., Yang, Q., Li, H., Luo, Y., Fang, C., Chen, J., Yang, X., Li, B., 2013. Responses of ecosystem carbon cycle to experimental warming: a meta-analysis. Ecology 94, 726–738.

Marschner, B., Brodowski, S., Dreves, A., Gleixner, G., Gude, A., Grootes, P.M., Hamer, U., Heim, A., Jandl, G., Ji, R., Kaiser, K., Kalbitz, K., Kramer, C., Leinweber, P., Rethemeyer, J., Schäffer, A., Schmidt, M.W.I., Schwark, L., Wiesenberg, G.L.B., 2008. How relevant is recalcitrance for the stabilization of organic matter in soils? Journal of Plant Nutrition and Soil Science 171 (1), 91–110.

Melillo, J.M., Frey, S.D., DeAngelis, K.M., Werner, W.J., Bernard, M.J., Bowles, F.P., Pold, G., Knorr, M.A., Grandy, A.S., 2017. Long-term pattern and magnitude of soil carbon feedback to the climate system in a warming world. Science 358, 101–105.

Morrison, E.W., Pringle, A., van Diepen, L.T.A., Grandy, A.S., Melillo, J.M., Frey, S.D., 2019. Warming alters fungal communities and litter chemistry with implications for soil carbon stocks. Soil Biology and Biochemistry 132, 120–130.

Müller, K., Kramer, S., Haslwimmer, H., Marhan, S., Scheunemann, N., Butenschön, O., Scheu, S., Kandeler, E., 2016. Carbon transfer from maize roots and litter into bacteria and fungi depends on soil depth and time. Soil Biology and Biochemistry 93, 79–89.

Niemeyer, J., Chen, Y., Bollag, J.-M., 1992. Characterization of humic acids, composts, and peat by diffuse reflectance Fourier-transform infrared spectroscopy. Soil Science Society of America Journal 56, 135–140.

Otto, A., Simpson, M.J., 2005. Degradation and preservation of vascular plant-derived biomarkers in grassland and forest soils from Western Canada. Biogeochemistry 74, 377–409.

Parts, K., Tedersoo, L., Schindlbacher, A., Sigurdsson, B.D., Leblans, N.I.W., Oddsdóttir, E.S., Borken, W., Ostonen, I., 2019. Acclimation of fine root systems to soil warming: comparison of an experimental setup and a natural soil temperature gradient. Ecosystems 22, 457–472.

Pendall, E., Bridgham, S., Hanson, P.J., Hungate, B., Kicklighter, D.W., Johnson, D.W., Law, B.E., Luo, Y., Megonigal, J.P., Olsrud, M., Ryan, M.G., Wan, S., 2004. Below-ground process responses to elevated CO_2 and temperature: a discussion of observations, measurement methods, and models. New Phytologist 162, 311–322.

Pisani, O., Frey, S.D., Simpson, A.J., Simpson, M.J., 2015. Soil warming and nitrogen deposition alter soil organic matter composition at the molecular-level. Biogeochemistry 123, 391–409.

Pold, G., Melillo, J.M., DeAngelis, K.M., 2015. Two decades of warming increases diversity of a potentially lignolytic bacterial community. Frontiers in Microbiology 6, 480.

Pold, G., Grandy, A.S., Melillo, J.M., DeAngelis, K.M., 2017. Changes in substrate availability drive carbon cycle response to chronic warming. Soil Biology and Biochemistry 110, 68–78.

Rasmussen, C., Torn, M.S., Southard, R.J., 2005. Mineral assemblage and aggregates control carbon dynamics in a California conifer forest. Soil Science Society of America Journal 69, 1711–1721.

Rasse, D.P., Rumpel, C., Dignac, M.F., 2005. Is soil carbon mostly root carbon? Mechanisms for a specific stabilisation. In: Plant and Soil, pp. 341–356.

Riederer, M., Matzke, K., Ziegler, F., Kögel-Knabner, I., 1993. Occurrence, distribution and fate of the lipid plant biopolymers cutin and suberin in temperate forest soils. Organic Geochemistry 20, 1063–1076.

Rillig, M.C., Wright, S.F., Shaw, M.R., Field, C.B., 2002. Artificial climate warming positively affects arbuscular mycorrhizae but decreases soil aggregate water stability in an annual grassland. Oikos 97, 52–58.

Rumpel, C., Kögel-Knabner, I., Bruhn, F., 2002. Vertical distribution, age, and chemical composition of organic carbon in two forest soils of different pedogenesis. Organic Geochemistry 33, 1131–1142.

Rumpel, C., Chabbi, A., Marschner, B., 2012. Carbon storage and sequestration in subsoil horizons: knowledge, gaps and potentials. In: Recarbonization of the Biosphere. Springer Netherlands, Dordrecht, pp. 445–464.

Schnecker, J., Borken, W., Schindlbacher, A., Wanek, W., 2016. Little effects on soil organic matter chemistry of density fractions after seven years of forest soil warming. Soil Biology and Biochemistry 103, 300–307.

Sokol, N.W., Sanderman, J., Bradford, M.A., 2018. Pathways of mineral-associated soil organic matter formation: integrating the role of plant carbon source, chemistry, and point-of-entry. Global Change Biology 25, 12–24. https://doi.org/10.1111/gcb.14482.

Solly, E.F., Lindahl, B.D., Dawes, M.A., Peter, M., Souza, R.C., Rixen, C., Hagedorn, F., 2017. Experimental soil warming shifts the fungal community composition at the alpine treeline. New Phytologist 215, 766–778.

Song, J., Wan, S., Piao, S., Knapp, A.K., Classen, A.T., Vicca, S., Ciais, P., Hovenden, M.J., Leuzinger, S., Beier, C., Kardol, P., Xia, J., Liu, Q., Ru, J., Zhou, Z., Luo, Y., Guo, D., Adam Langley, J., Zscheischler, J., Dukes, J.S., Tang, J., Chen, J., Hofmockel, K.S., Kueppers, L.M., Rustad, L., Liu, L., Smith, M.D., Templer, P.H., Quinn Thomas, R., Norby, R.J., Phillips, R.P., Niu, S., Fatichi, S., Wang, Y., Shao, P., Han, H., Wang, D., Lei, L., Wang, J., Li, Xiaona, Zhang, Q., Li, Xiaoming, Su, F., Liu, B., Yang, F., Ma, G., Li, G., Liu, Yanchun, Liu, Yinzhan, Yang, Z., Zhang, K., Miao, Y., Hu, M., Yan, C., Zhang, A., Zhong, M., Hui, Y., Li, Y., Zheng, M., 2019. A meta-analysis of 1,119 manipulative experiments on terrestrial carbon-cycling responses to global change. Nature Ecology and Evolution 3, 1309–1320.

Soong, J.L., Castanha, C., Hicks Pries, C.E., Ofiti, N.O.E., Porras, R.C., Riley, W.J., Schmidt, M.W.I., Torn, M.S., 2021. Five years of whole-soil warming led to loss of subsoil carbon stocks and increased CO_2 efflux. Science Advances. Submitted for publication.

Soong, J.L., Fuchslueger, L., Marañon-Jimenez, S., Torn, M.S., Janssens, I.A., Penuelas, J., Richter, A., 2020a. Microbial carbon limitation: the need for integrating microorganisms into our understanding of ecosystem carbon cycling. Global Change Biology 26, 1953–1961.

Soong, J.L., Phillips, C.L., Ledna, C., Koven, C.D., Torn, M.S., 2020b. CMIP5 models predict rapid and deep soil warming over the 21st century. Journal of Geophysical Research: Biogeosciences 125. https://doi.org/10.1029/2019JG005266.

van Gestel, N., Shi, Z., van Groenigen, K.J., Osenberg, C.W., Andresen, L.C., Dukes, J.S., Hovenden, M.J., Luo, Y., Michelsen, A., Pendall, E., Reich, P.B., Schuur, E.A.G., Hungate, B.A., 2018. Predicting soil carbon loss with warming. Nature 554, E4–E5.

Vaughn, L.J.S., Torn, M.S., 2019. ^{14}C evidence that millennial and fast-cycling soil carbon are equally sensitive to warming. Nature Climate Change 9, 467–471.

Wan, S., Norby, R.J., Pregitzer, K.S., Ledford, J., O'Neill, E.G., 2004. CO_2 enrichment and warming of the atmosphere enhance both productivity and mortality of maple tree fine roots. New Phytologist 162, 437–446.

Wang, P., Limpens, J., Mommer, L., van Ruijven, J., Nauta, A.L., Berendse, F., Schaepman-Strub, G., Blok, D., Maximov, T.C., Heijmans, M.M.P.D., 2017. Above-and below-ground responses of four tundra plant functional types to deep soil heating and surface soil fertilization. Journal of Ecology 105, 947–957.

Wiesenberg, G.L.B., Gocke, M.I., 2017. Analysis of lipids and polycyclic aromatic hydrocarbons as indicators of past and present (micro)biological activity. In: McGenity, T.J., Timmis, K.N., Nogales, B. (Eds.), Hydrocarbon and Lipid Microbiology Protocols: Petroleum, Hydrocarbon and Lipid Analysis. Springer Berlin Heidelberg, Berlin, Heidelberg, pp. 61–91.

Wiesenberg, G.L.B., Dorodnikov, M., Kuzyakov, Y., 2010. Source determination of lipids in bulk soil and soil density fractions after four years of wheat cropping. Geoderma 156, 267–277.

Zhao, Z., Dong, S., Jiang, X., Zhao, J., Liu, S., Yang, M., Han, Y., Sha, W., 2018. Are land use and short time climate change effective on soil carbon compositions and their relationships with soil properties in alpine grassland ecosystems on Qinghai-Tibetan Plateau? The Science of the Total Environment 625, 539–546.

R Core Team (2020). R: A language and environment for statistical computing. R Foundation for Statistical Computing, Vienna, Austria. URL https://www.R-project.org/.

RStudio Team (2019). RStudio: Integrated Development for R. RStudio, PBC, Boston, MA URL http://www.rstudio.com/.